

# Geometric Properties of the Three-Dimensional Ising and XY Models

Frank Winter,<sup>1,\*</sup> Wolfhard Janke,<sup>2</sup> and Adriaan M. J. Schakel<sup>1</sup>

<sup>1</sup>*Institut für Theoretische Physik, Freie Universität Berlin,  
Arnimallee 14, 14195 Berlin, Germany*

<sup>2</sup>*Institut für Theoretische Physik, Universität Leipzig,  
Postfach 100920, 04009 Leipzig, Germany*

(Dated: August 29, 2021)

## Abstract

The fractal structure of high-temperature graphs of the three-dimensional Ising and XY models is investigated by simulating these graphs directly on a cubic lattice and analyzing them with the help of percolation observables. The Ising graphs are shown to percolate right at the Curie critical point. The diverging length scale relevant to the graphs in the vicinity of the percolation threshold is shown to be provided by the spin correlation length. The fractal dimension of the high-temperature graphs at criticality is estimated to be  $D = 1.7349(65)$  for the Ising and  $D = 1.7626(66)$  for the XY model.

---

\*Present address: Deutsches Elektronen-Synchrotron DESY, Platanenallee 6, 15738 Zeuthen, Germany

## I. INTRODUCTION

The high-temperature (HT) expansion is a powerful tool to study the critical properties of lattice spin models [1]. In this approach, the partition function and correlation functions are calculated by counting graphs on the lattice with each graph representing a certain contribution. Traditionally, such an expansion is carried out exactly to a given order by enumerating all possible ways a graph of given size and topology can be drawn on the lattice. This exact approach, involving combinatorial and graph-theoretical algorithms, is notoriously challenging and laborious, with each additional order requiring typically about the same amount of effort needed for all previous orders combined.

We have developed a different approach [2] in which the HT representation of lattice spin models is studied by means of Monte Carlo simulations. The HT graphs along the links of the underlying lattice are generated through a Metropolis plaquette update that proposes a local change in the existing graph configuration. At high temperatures, only a few small graphs generated this way can be found scattered throughout the lattice. As the temperature is lowered, graphs start to fill the lattice by growing larger and becoming more abundant. At temperatures below the critical temperature, the lattice becomes filled with graphs. A typical graph configuration now consists of one big graph spanning the entire lattice and a collection of much smaller graphs (see Fig. 1). The steady increase in the number of occupied links and the appearance of graphs spanning the lattice as the temperature is lowered are reminiscent of a percolation process. The use of percolation observables therefore suggests itself to analyze the graph configurations. For these observables to have bearing on the critical properties of the model under investigation, it is necessary that the HT graphs percolate right at the thermal critical point. For the Ising model on a square lattice we numerically showed that the percolation threshold indeed coincides with the (exactly known) Curie temperature [2]. In other words, the phase transition in this lattice spin model to the ordered, low-temperature state manifests itself through a proliferation of HT graphs. Moreover, the fractal structure of closed and open graphs was shown to encode the standard critical exponents [2, 3, 4, 5].

The purpose of this paper is to extend this geometric Monte Carlo approach to three dimensions. Two-dimensional (2D) spin models arguably form a very special class of models, in particular the Ising model as it is self-dual. It therefore is *a priori* not obvious that this geometric Monte Carlo approach together with the use of percolation observables is viable

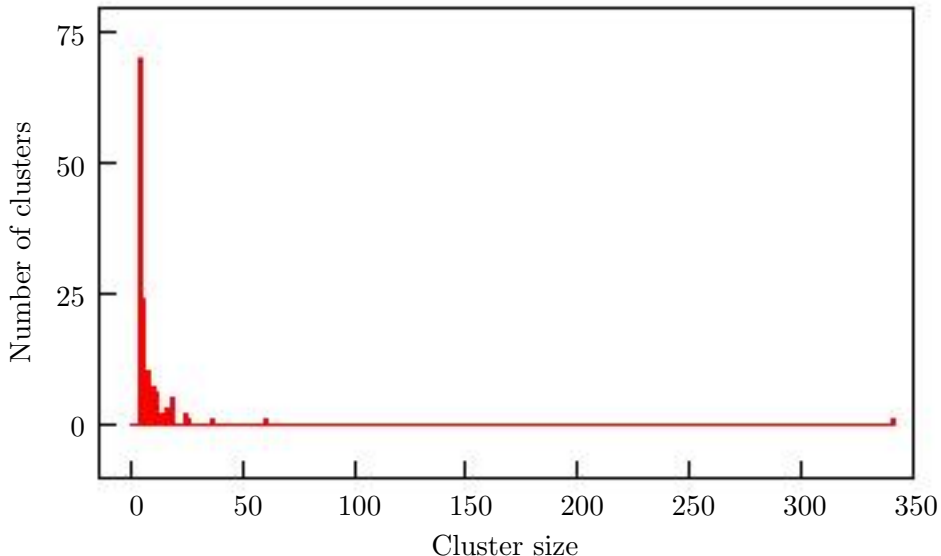


FIG. 1: Distribution of Ising HT graphs on a cubic lattice of linear size  $L = 24$  at the percolation threshold. Note the presence of a single big graph and many much smaller graphs.

in 3D.

Another Monte Carlo algorithm for studying HT representations of classical statistical models has been put forward by Prokof'ev and Svistunov [6]. That so-called worm algorithm is much more efficient than the conventional local update we use. The dynamic exponent  $z$  characterizing the divergence of the autocorrelation time  $\tau$  when the critical point is approached,  $\tau \sim \xi^z$ , with  $\xi$  the correlation length, is close to zero for the worm algorithm while it is larger than two for the plaquette update we use. The plaquette update, on the other hand, has the virtue that it provides a direct and clean implementation of the HT representations of the spin models we consider. Prokof'ev and Svistunov [4] recently applied their algorithm to the 3D complex  $|\phi|^4$  theory to determine the fractal dimension of the HT graphs in that theory. These graphs are unlike those in the XY model as links and vertices carry different weights in the two models. Moreover, because the update algorithms differ, the graphs in the two models are simulated in completely different ways. Nevertheless, since the  $|\phi|^4$  theory is in the same universality class as the XY model, both types of HT graphs should yield the same fractal dimension. We set out below to investigate whether universality holds for the fractal structure of HT graphs.

The paper is organized as follows. The next section introduces the Metropolis plaquette

update algorithm used in this Monte Carlo study together with the percolation observables applied to analyze the HT graphs. The subsequent two sections present our results for the Ising (Sec. III) and XY (Sec. IV) models, and the paper ends in Sec. V with a summary and conclusions.

## II. SIMULATION AND DATA ANALYSIS TECHNIQUES

To be specific, we consider the HT representation of  $O(N)$  lattice spin models described by the Hamiltonian

$$H = -J \sum_{\langle \mathbf{x}, \mathbf{x}' \rangle} \mathbf{S}_{\mathbf{x}} \cdot \mathbf{S}_{\mathbf{x}'}, \quad (1)$$

with the interaction, characterized by the parameter  $J$ , restricted to spins on nearest-neighbor sites, so that the sum in Eq. (1) runs only over nearest-neighbor pairs. The spin variable  $\mathbf{S}_{\mathbf{x}} = (S_{\mathbf{x}}^1, \dots, S_{\mathbf{x}}^N)$  located at each site  $\mathbf{x}$  of the cubic lattice has a fixed length,  $\mathbf{S}_{\mathbf{x}}^2 = 1$ . Simulations are carried out for the 3D Ising ( $N = 1$ ) and XY ( $N = 2$ ) models.

### A. Ising Model

The HT representation of the 3D Ising model on a cubic lattice with periodic boundary conditions consisting of  $N$  sites and  $3N$  links [7],

$$Z = (\cosh \beta)^{3N} 2^N \sum_{\substack{\text{closed} \\ \text{graphs}}} K^b, \quad (2)$$

provides an alternative, but completely equivalent description of the spin model. In this representation, which is purely geometric in nature, spin degrees of freedom are swapped for link variables. The representation (2) of the partition function can be visualized as a sum over all possible closed graphs that can be drawn on the lattice. Each occupied link carries a factor  $K = \tanh \beta$ , with  $\beta$  the inverse temperature, where for convenience the coupling constant  $J$  is set to unity. In the entire temperature range  $0 \leq \beta \leq \infty$ ,  $0 \leq K \leq 1$ . The minimum number of occupied links  $b$  needed to form a closed graph is four on a cubic lattice.

The internal energy

$$E = -\frac{\partial \ln Z}{\partial \beta} = -3NK - \frac{1}{\sinh \beta \cosh \beta} \langle b \rangle \quad (3)$$

is determined by the average number  $\langle b \rangle$  of occupied links.

The central idea of our geometric Monte Carlo approach [2] is to directly simulate the graphs contributing to the partition function. The HT representation (2) suggests the following local Metropolis update algorithm [8].

The probability distribution  $P(G)$  for a given graph configuration  $G$  reads in equilibrium

$$P(G) = \frac{1}{Z} (\cosh \beta)^{3N} 2^N K^b. \quad (4)$$

Such a configuration can be reached from the configuration present after, say,  $t$  iterations in the following way

$$P_{t+1}(G) = P_t(G) + \sum_{G'} [P_t(G')W(G' \rightarrow G) - P_t(G)W(G \rightarrow G')], \quad (5)$$

where  $W(G \rightarrow G')$  is the probability for the system to move from the graph configuration  $G$  with  $b$  occupied links to the graph configuration  $G'$  with  $b'$  occupied links. In equilibrium,  $P_{t+1}(G) = P_t(G) = P(G)$ , and the system satisfies detailed balance

$$P(G')W(G' \rightarrow G) = P(G)W(G \rightarrow G'), \quad (6)$$

or

$$\frac{W(G \rightarrow G')}{W(G' \rightarrow G)} = \frac{P(G')}{P(G)} = \frac{K^{b'}}{K^b}. \quad (7)$$

As is custom with Metropolis algorithms, the acceptance rate  $p_{\text{HT}}$  of a proposed update is maximized by giving the largest of the two transition probabilities  $W(G \rightarrow G')$  and  $W(G' \rightarrow G)$  appearing in the ratio the largest possible value, which is one. That is, if the number of links  $b'$  in the proposed configuration is larger than the number of links  $b$  in the existing configuration, so that  $K^{b'}/K^b < 1$ ,  $W(G' \rightarrow G) = 1$  and  $W(G \rightarrow G') = p_{\text{HT}}$ . If, on the other hand,  $b' < b$ , the proposed configuration carries a larger weight than the existing one and will always be accepted.

The HT graphs are generated by taking the smallest possible closed graphs on the lattice, i.e., plaquettes, as building blocks. During a sweep of the lattice, all plaquettes are visited in a regular, typewriter fashion. For the Ising model, reflecting the underlying  $Z_2$  spin symmetry, a link can either be empty or occupied. The links of a plaquette considered for update are changed from empty to occupied and *vice versa* (see Fig. 2 for an illustration). This is easily implemented by means of the binary rules  $0 + 1 = 1$ ,  $1 + 1 = 0$ , respectively. The acceptance rate of a proposed update reads in formula [8]

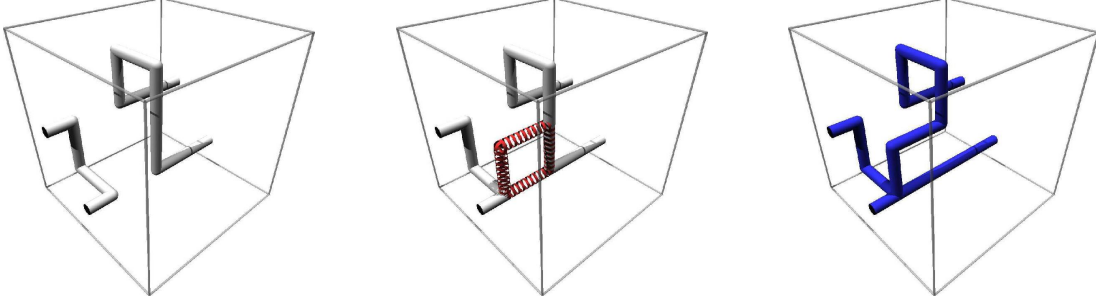


FIG. 2: An existing Ising HT graph on a cubic lattice (left panel) is updated with the help of a chosen plaquette (middle panel) into a new graph (right panel).

$$p_{\text{HT}} = \begin{cases} K^{b'-b} & \text{if } b' > b \\ 1 & \text{else.} \end{cases} \quad (8)$$

The resulting and existing number of occupied links,  $b'$  and  $b$ , respectively, are related via

$$b' = b + 4 - 2b_{\square}, \quad (9)$$

with  $b_{\square}$  denoting the number of links on the plaquette already occupied. By taking plaquettes as building blocks, the resulting graphs are automatically closed.

Table I gives a summary of the number  $N_{\text{MC}}$  of Monte Carlo sweeps of the lattice of size  $L$  used for data collection in the temperature interval  $[\beta_1, \beta_2]$ , with  $N_{\text{cal}}$  sweeps used for equilibration. The temperature intervals are sampled with  $i$  equidistant points. The largest lattice taken for temperature-dependent runs is  $L = 48$ , while runs at the percolation threshold are carried out on lattices up to  $L = 64$ . Since the plaquette update is a local update, autocorrelation times grow very large on large lattices. Analyzing the time series of the percolation strength, we estimate the autocorrelation time to vary from  $\tau \approx 25$  for  $L = 10$  to as long as  $\tau \approx 2500$  for  $L = 64$ . To somewhat reduce correlations between successive data points, we take measurements every fifth sweep of the lattice. Statistical errors are estimated by means of jackknife binning. Fits are carried out by using the nonlinear Marquardt-Levenberg algorithm for minimization of error weighted least squares.

TABLE I: Overview of parameters used in the simulations of the 3D Ising model. The temperature intervals  $[\beta_1, \beta_2]$  are sampled with  $i$  equidistant points. For each sampling point,  $N_{\text{MC}}$  Monte Carlo sweeps of the lattice of size  $L$  are used for data collection, with  $N_{\text{cal}}$  sweeps used for equilibration.

$\beta_1$	$\beta_2$	$i$	$L$	$N_{\text{MC}}$	$N_{\text{cal}}$
0.218000	0.233000	70	12	460000	60000
0.170000	0.218000	190	12	120000	20000
0.233000	0.270000	120	12	120000	20000
0.220000	0.230000	60	16	460000	60000
0.170000	0.220000	190	16	120000	20000
0.230000	0.270000	140	16	120000	20000
0.220500	0.229000	50	20	460000	60000
0.170000	0.220500	190	20	120000	20000
0.229000	0.270000	150	20	120000	20000
0.220500	0.227100	40	24	460000	60000
0.170000	0.220500	190	24	120000	20000
0.227100	0.270000	160	24	120000	20000
0.220500	0.226000	35	28	460000	80000
0.170000	0.220500	180	28	120000	30000
0.226000	0.270000	165	28	120000	30000
0.220500	0.224900	30	32	460000	80000
0.170000	0.220500	190	32	120000	30000
0.224900	0.270000	170	32	120000	30000
0.220500	0.223800	25	40	500000	120000
0.170000	0.220500	180	40	130000	40000
0.223800	0.270000	175	40	130000	40000
0.220500	0.223500	25	48	560000	240000
0.170000	0.220500	150	48	140000	50000
0.223500	0.270000	160	48	140000	50000

## B. XY Model

For the XY model ( $N = 2$ ), where the spins take values along a circle, the general spin Hamiltonian (1) with  $J = 1$  reduces to

$$H = - \sum_{\langle \mathbf{x}, \mathbf{x}' \rangle} \cos(\theta_{\mathbf{x}} - \theta_{\mathbf{x}'}), \quad (10)$$

with  $\theta_{\mathbf{x}}$  being the planar angle of the spin at site  $\mathbf{x}$  relative to a fixed, but arbitrary axis. The HT expansion is facilitated by the use of the Fourier expansion

$$e^{\beta \cos(\theta)} = \sum_{l=-\infty}^{\infty} I_l(\beta) e^{il\theta}, \quad (11)$$

where  $I_l(x)$  is the modified Bessel function of the first kind. The partition function,

$$Z = \prod_{\mathbf{x}} \left[ \int_{-\pi}^{\pi} \frac{d\theta_{\mathbf{x}}}{2\pi} \right] \prod_{\langle \mathbf{x}, \mathbf{x}' \rangle} e^{-\beta \cos(\theta_{\mathbf{x}} - \theta_{\mathbf{x}'})} \quad (12)$$

then takes the well-known form [9]

$$Z = \prod_{\mathbf{x}} \left[ \int_{-\pi}^{\pi} \frac{d\theta_{\mathbf{x}}}{2\pi} \right] \prod_{\langle \mathbf{x}, \mathbf{x}' \rangle} \sum_{l_{\mathbf{x}, \mathbf{x}'}} I_{l_{\mathbf{x}, \mathbf{x}'}}(\beta) e^{il_{\mathbf{x}, \mathbf{x}'}(\theta_{\mathbf{x}} - \theta_{\mathbf{x}'}),} \quad (13)$$

involving the integers  $l_{\mathbf{x}, \mathbf{x}'}$  defined on the links connecting the nearest neighbor sites  $\mathbf{x}$  and  $\mathbf{x}'$ . The spin degrees of freedom are now easily integrated out with the result

$$Z = \prod_{\langle \mathbf{x}, \mathbf{x}' \rangle} \sum'_{l_{\mathbf{x}, \mathbf{x}'}} I_{l_{\mathbf{x}, \mathbf{x}'}}(\beta) = I_0^{3N}(\beta) \prod_{\langle \mathbf{x}, \mathbf{x}' \rangle} \left( 1 + \sum_{l_{\mathbf{x}, \mathbf{x}' \neq 0}} \frac{I_{l_{\mathbf{x}, \mathbf{x}'}}(\beta)}{I_0(\beta)} \right). \quad (14)$$

Here, the prime on the sums is to indicate that only configurations satisfying the zero divergence condition,  $\sum_{\mathbf{x}'} l_{\mathbf{x}, \mathbf{x}'} = 0$  at each site  $\mathbf{x}$  contribute, where the sum  $\sum_{\mathbf{x}'}$  runs over all nearest neighbors of  $\mathbf{x}$ . It is generally accepted that the link variables  $l_{\mathbf{x}, \mathbf{x}'}$  at the right hand of Eq. (14) can be restricted to the values  $\pm 1$  without changing the universality class. The partition function of the XY model can then be cast in a form analogous to the HT representation (2) of the Ising model,

$$Z = I_0^{3N}(\beta) \sum_{\substack{\text{closed} \\ \text{oriented graphs}}} K^b, \quad (15)$$

where  $K \equiv I_1(\beta)/I_0(\beta)$ , with  $0 \leq K < 1$  for all  $\beta$ , and use is made of the property that  $I_{-1}(x) = I_1(x)$ . Since the link variable of the truncated model can take two nontrivial

values  $\pm 1$ , the graphs now have, in contrast to the Ising model, an orientation. A plaquette considered for update must therefore also be given a (randomly chosen) orientation. As binary rules we now have  $-1 + 1 = 0$ ,  $0 + 1 = 1$ ,  $0 - 1 = -1$ ,  $1 - 1 = 0$  in addition to the restrictions  $-1 - 1 = 0$ ,  $1 + 1 = 0$  of singly occupancy which, as already mentioned, we expect not to change the universality class of the model. Apart from these modifications, the HT representation of the XY model can be handled in the same way as that of the Ising model.

### C. Observables

The HT graphs are analyzed with the help of standard percolation observables [10]. An important characteristic is whether a graph spans the lattice or not. We say a graph does so already if it spans the lattice in just one of the three possible directions. By recording this each time the graphs are analyzed, one obtains the percolation probability  $P_S$ , which tends to zero in the limit  $\beta \rightarrow 0$  and to unity in the opposite limit  $\beta \rightarrow \infty$ . Another important observable is the graph distribution  $n_b$ , which gives the average number of graphs of  $b$  occupied links normalized by the volume. Close to the percolation threshold it assumes the form

$$n_b \sim b^{-\tau} e^{-\theta b}, \quad \theta \propto |K/K_{\text{per}} - 1|^{1/\sigma}. \quad (16)$$

The exponents  $\tau$  and  $\sigma$  are related to the fractal dimension  $D$  of the HT graphs via  $\tau = d/D + 1$  with  $d = 3$  the dimension of the space box, and [3]

$$\sigma = 1/\nu D, \quad (17)$$

where  $\nu$  is the exponent characterizing the divergence of the correlation length  $\xi$  as the percolation threshold is approached,  $\xi \propto |K/K_{\text{per}} - 1|^{-\nu}$ . An additional observable we measure is the percolation strength  $P_\infty$ , which is defined as the size of the largest graph normalized by the volume. Finally, we also record the average graph size  $\chi_G$ .

The percolation threshold and the fractal dimension of the HT graphs follow from applying finite-size scaling to these observables. According to scaling theory, the percolation probability and strength for different values of the tuning parameter  $K$  and for different lattice sizes  $L$  do not depend on these variables separately, but depend on them in a convoluted

way [11]

$$P_S(K) = P_S [L^{1/\nu}(K/K_{\text{per}} - 1)] , \quad P_\infty(K) = L^{-\beta_G/\nu} P_\infty [L^{1/\nu}(K/K_{\text{per}} - 1)] . \quad (18)$$

Here,  $\beta_G$  determines the scaling dimension of the percolation strength, which is related to the fractal dimension  $D$  of the HT graphs through [10]

$$D = d - \beta_G/\nu. \quad (19)$$

The scaling dimension of the percolation probability is zero. The first scaling relation in Eq. (18) implies that the curves  $P_S(K)$  measured on lattices of different size all cross at the same point. This point, being volume independent, marks the percolation threshold  $K_{\text{per}}$  on the infinite lattice. That scaling relation in addition implies that the curves collapse onto a universal curve when replotted as a function of  $L^{1/\nu}(K/K_{\text{per}} - 1)$ . Similarly, the second scaling relation in Eq. (18) implies that if in addition to the horizontal axis also the vertical axis is properly rescaled, with the correct value for the ratio  $\beta_G/\nu$ , also the  $P_\infty(K)$  data fall onto a universal curve. That scaling relation in addition implies that measurements at the percolation threshold scale as  $P_\infty(K_{\text{per}}) \propto L^{-\beta_G/\nu}$ , providing a good means of determining  $\beta_G/\nu$ .

### III. ISING MODEL RESULTS

We start by simulating the HT graphs of the Ising model on a cubic lattice. Figure 3 shows the internal energy as obtained through Eq. (3) by measuring the density of occupied links. Apart from a small interval around the critical temperature,  $E$  is seen to be almost independent of volume, implying that the correlation length is much smaller here than the linear size of the smallest lattice considered ( $L = 12$ ). When entering the critical region, the correlation length becomes larger and eventually exceeds the size of the largest lattice considered ( $L = 48$ ).

We first determine the location of the percolation threshold. To this end, we measure the percolation probability on lattices of different linear size  $L$  as a function of the inverse temperature (see Fig. 4). The figure shows that the curves connecting the data points all cross within error bars at the critical temperature, giving a first indication that the percolation threshold coincides with the thermal critical point. The percolation probability

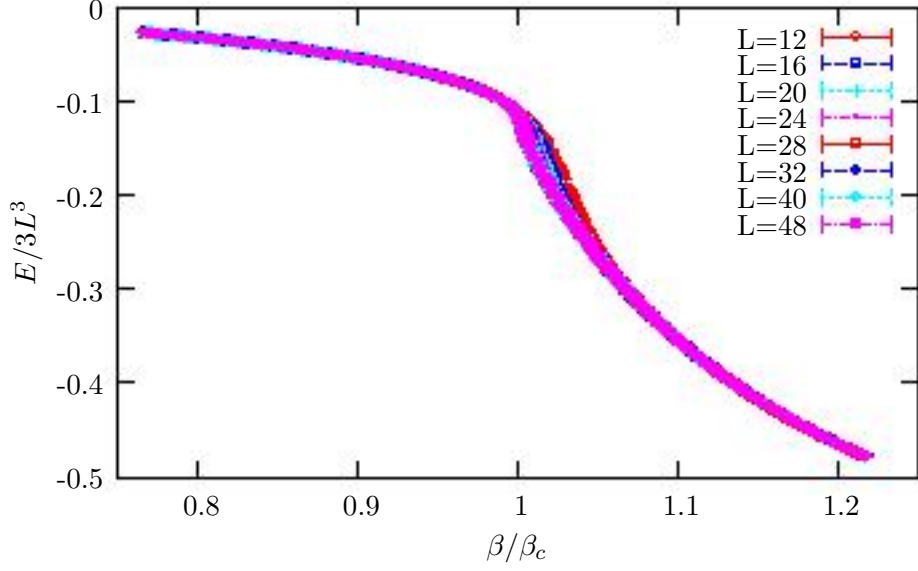


FIG. 3: Average Ising HT graph density as a function of the reduced inverse temperature  $\beta/\beta_c$  for cubic lattices varying in linear size from  $L = 12$  to  $L = 48$ .

at the threshold we estimate to be  $P_S = 0.05(2)$ . To obtain a more refined test, we apply finite-size scaling to this observable. When replotted as a function of  $(\beta/\beta_c - 1)L^{1/\nu}$ , with  $\nu$  the correlation length exponent of the 3D Ising model, the data is expected to collapse onto a universal curve. The inverse critical temperature and  $\nu$  have been determined to high precision in Refs. [12, 13],

$$\beta_c = 0.22165459(10), \quad \nu = 0.63012(16), \quad (20)$$

respectively. Figure 5 shows that these values indeed produce a good collapse of the data in the entire temperature range. Since this is achieved without any adjustable parameter, we arrive at the important conclusion that the percolation threshold of the HT graphs coincides within error bars with the thermal critical point. Moreover, since the standard Ising correlation length exponent  $\nu$  has been used, it follows that the relevant diverging length scale for the HT graphs in the vicinity of the critical temperature is provided by the spin correlation length.

We proceed to determine the fractal dimension  $D$  of the HT graphs. This can be done by measuring, for example, the percolation strength or the average graph size at the percolation threshold and applying finite-size scaling to the data obtained for different lattice sizes  $L$ . Since  $\chi_G$  was found to show large corrections to scaling for small  $L$ , the observable  $P_\infty$ ,

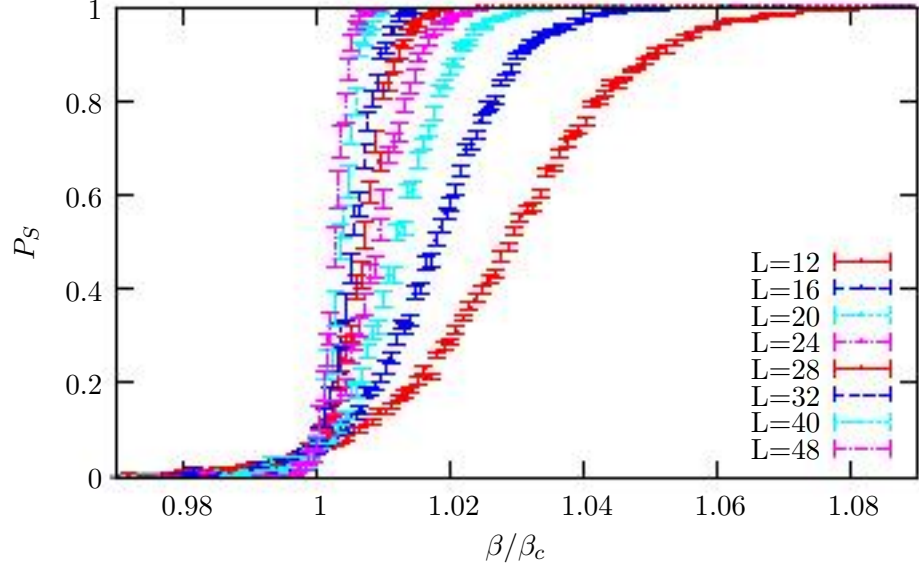


FIG. 4: Percolation probability  $P_S$  of the Ising HT graphs as a function of the reduced inverse temperature  $\beta/\beta_c$  for cubic lattices varying in linear size from  $L = 12$  to  $L = 48$ .

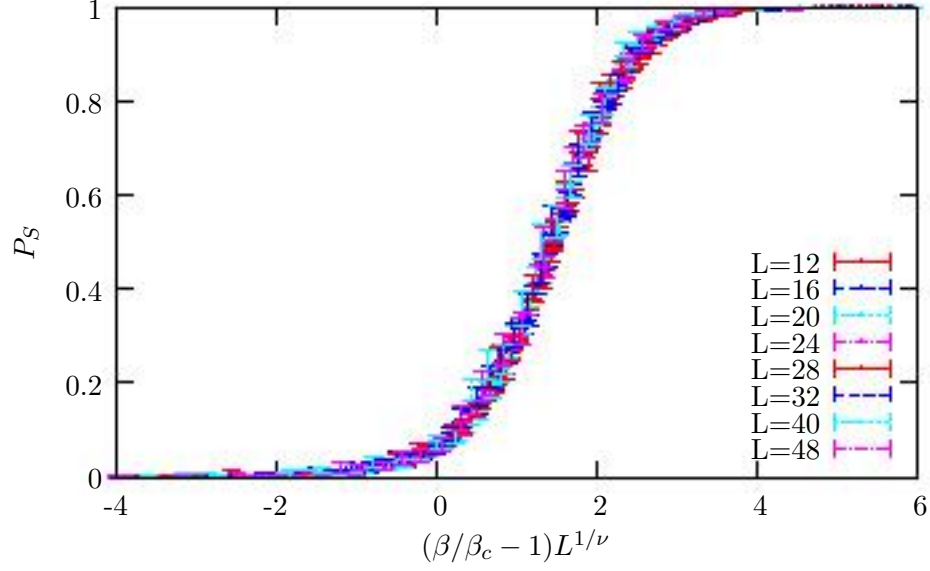


FIG. 5: Collapse of the data in Fig. 4 with the choices (20) for  $\beta_c$  and  $\nu$ .

showing only small corrections, is used to estimate  $D$ . Table II summarizes the results of two-parameter fits using the nonlinear Marquardt-Levenberg algorithm for various fit intervals. On the basis of these fits, we estimate the critical exponent  $\beta_G/\nu$  to be

TABLE II: Percolation strength exponent  $\beta_G/\nu$  of the Ising HT graphs at the critical temperature (20) as obtained through two-parameter fits in the indicated intervals.

$L$	$\beta_G/\nu$	$\chi^2/\text{DOF}$	$L$	$\beta_G/\nu$	$\chi^2/\text{DOF}$
8 – 64	1.256(5)	1.61	10 – 64	1.265(7)	1.35
8 – 56	1.255(6)	1.68	10 – 56	1.264(7)	1.43
8 – 48	1.255(6)	1.75	10 – 48	1.266(8)	1.43
8 – 40	1.258(6)	1.57	10 – 40	1.271(7)	0.96
8 – 32	1.254(7)	1.57	10 – 32	1.267(8)	1.05
8 – 24	1.253(7)	1.50	10 – 24	1.269(8)	0.85
8 – 20	1.245(8)	1.19	10 – 20	1.260(11)	0.83
12 – 64	1.256(5)	1.61	14 – 64	1.270(10)	1.41
12 – 56	1.270(9)	1.41	14 – 56	1.269(12)	1.53
12 – 48	1.273(9)	1.37	14 – 48	1.273(13)	1.51
12 – 40	1.281(7)	0.68	16 – 64	1.261(13)	1.37
12 – 32	1.279(9)	0.79	16 – 56	1.258(15)	1.47
12 – 24	1.285(7)	0.34	16 – 48	1.261(17)	1.49

$$\beta_G/\nu = 1.2651(65), \quad (21)$$

corresponding to the largest possible fit interval ( $L = 10 - 64$ ) that still gives a good fit quality with a  $\chi^2$  per degree of freedom (DOF),  $\chi^2/\text{DOF} = 1.35$ . Figure 7 shows that, with this choice, the data collected in the vicinity of the critical temperature on lattices of different size  $L$  fall onto a universal curve when both axes are properly rescaled.

The estimate (21) for the graph exponent leads to the estimate

$$D = d - \beta_G/\nu = 1.7349(65) \quad (22)$$

( $d = 3$ ) for the fractal dimension of the HT graphs at the critical point. This fractal dimension is closer to that of a self-avoiding walk in 3D, for which [14]  $D = 1/\nu = 1.7001(32)$ , than to that of a Brownian random walk, for which  $D = 2$ . Given this estimate for the fractal dimension, the relation (17) leads to the estimate

$$\sigma = 0.9147(42) \quad (23)$$

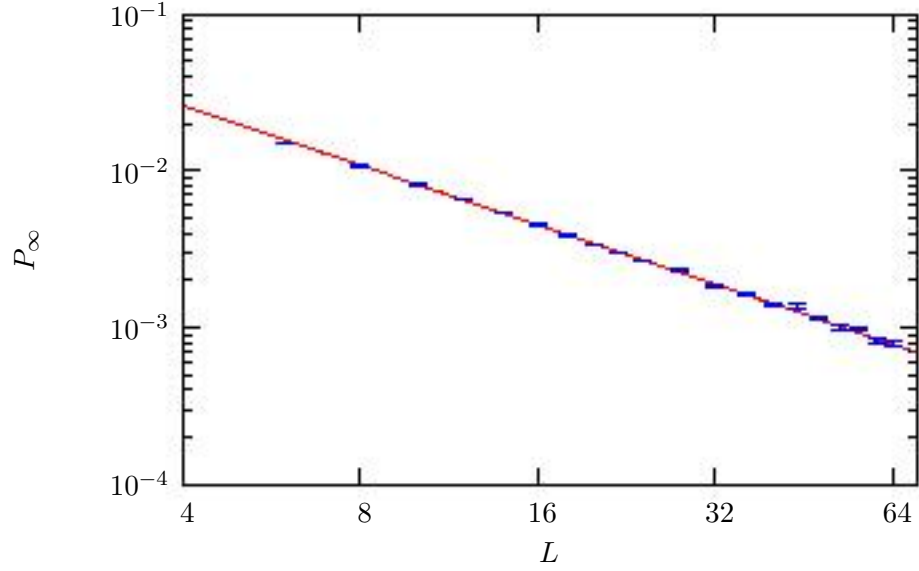


FIG. 6: Log-log plot of the percolation strength  $P_\infty$  of the Ising HT graphs at the critical temperature (20) as a function of the lattice size  $L$ . The straight line is obtained through a two-parameter fit in the interval  $L = 10 - 64$ .

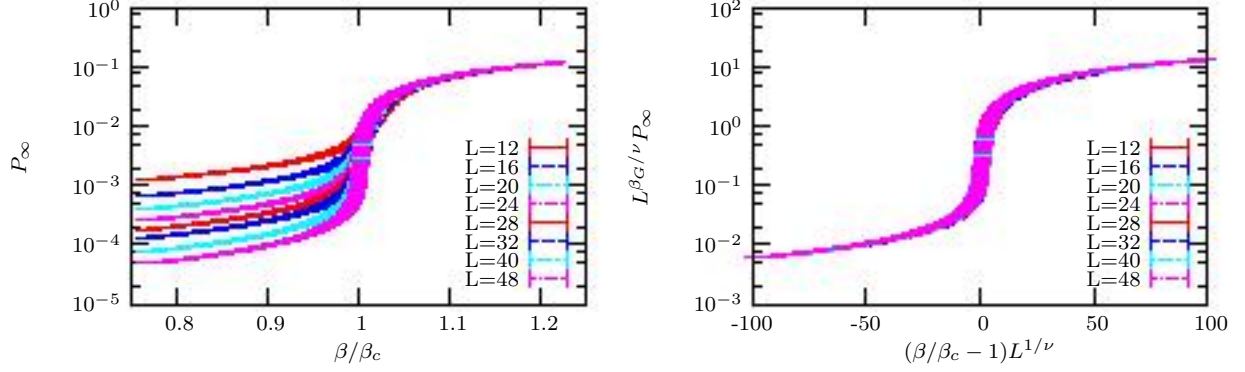


FIG. 7: Collapse of the Ising percolation strength data measured on lattices of different size  $L$  (left panel) when  $L^{\beta_G/\nu} P_\infty$  is plotted as a function of  $(\beta/\beta_c - 1)L^{1/\nu}$  (right panel) on a semilogarithmic scale.

for the graph distribution exponent  $\sigma$ , which for self-avoiding random walks is unity.

#### IV. XY MODEL RESULTS

We proceed by analyzing the HT graphs of the 3D XY model. The critical temperature of the truncated XY model, where links are allowed to be at most singly occupied, has to our knowledge not been determined before. To arrive at an accurate estimate of the percolation threshold, we consider the percolation strength data and search for the best data collapse given the value

$$\nu = 0.6717(1) \quad (24)$$

for the XY correlation length exponent recently reported in Ref. [15]. This is done by rendering a motion picture out of about 300 single frames showing the data collapse for different values of  $K_c$ . Successive frames correspond to slightly increased values of  $K_c$ . A media player, such as MPlayer that can go forward and backward frame by frame, is used to play the motion picture, and to determine the value of  $K_c$  with the best collapse. The quality of the collapse is established visually. Error estimates are based on the number of successive frames for which the quality of collapse remains roughly the same. We have checked this method by applying it to the Ising model, where the critical temperature is known to high precision, and obtained surprisingly good results. For the truncated XY model, we arrive in this way at the estimate

$$K_{\text{per}} = 0.22288(5), \quad (25)$$

which is to be compared to the value  $K_c = \tanh \beta_c = 0.218095 \dots$  of the Ising model. Figure 8 shows the collapse of the data achieved with the estimate (25) of the percolation threshold.

As for the Ising model, we determine the fractal dimension of the HT graphs of the XY model by measuring the percolation strength  $P_\infty$  at the percolation threshold (25) on lattices of different size. Table III summarizes the results of two-parameter fits using various fit intervals. On the basis of these fits, we estimate the critical exponent  $\beta_G/\nu$  to be

$$\beta_G/\nu = 1.2374(66), \quad (26)$$

corresponding to the largest possible fit interval ( $L = 10 - 64$ ) that still gives a good fit quality ( $\chi^2/\text{DOF} = 1.21$ ). Figure 10 shows that with this choice, the data collected in the vicinity of the percolation threshold on lattices of different size  $L$  fall onto a universal curve when both axes are properly rescaled. The result (26) leads to the estimate

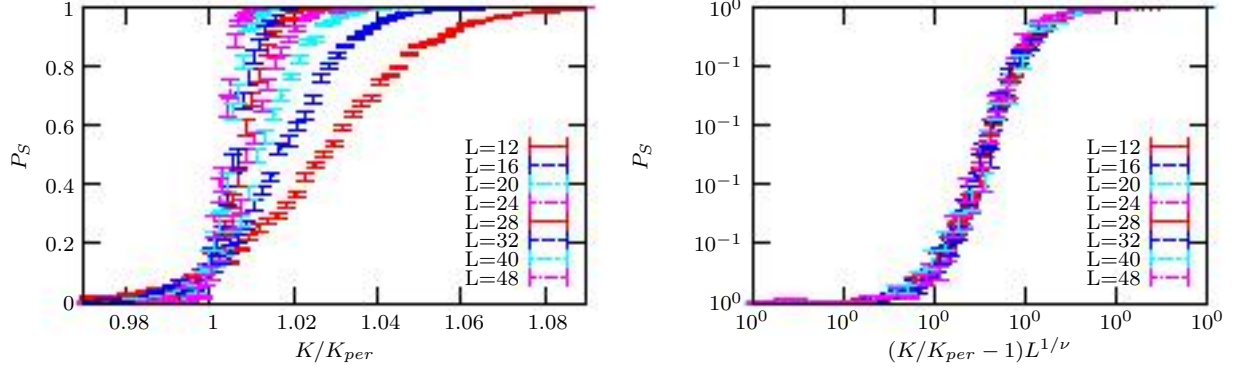


FIG. 8: Collapse of the percolation probability  $P_S$  of XY HT graphs measured on lattices of different size  $L$  (left panel) when replotted as a function of  $(K/K_{\text{per}} - 1)L^{1/\nu}$  (right panel).

TABLE III: Percolation strength exponent  $\beta_G/\nu$  of the XY HT graphs at the percolation threshold (25) as obtained through two-parameter fits in the indicated intervals.

$L$	$\beta_G/\nu$	$\chi^2/\text{DOF}$	$L$	$\beta_G/\nu$	$\chi^2/\text{DOF}$
6 – 64	1.203(7)	4.03	8 – 64	1.221(7)	2.34
6 – 56	1.200(7)	3.93	8 – 56	1.217(7)	2.36
6 – 48	1.196(6)	3.21	8 – 48	1.212(7)	1.85
6 – 40	1.192(6)	2.73	8 – 40	1.208(7)	1.60
6 – 32	1.188(7)	2.66	8 – 32	1.203(8)	1.71
6 – 24	1.185(7)	2.83	8 – 24	1.200(9)	1.98
6 – 20	1.179(8)	2.35	8 – 20	1.192(11)	1.95
$L$	$\beta_G/\nu$	$\chi^2/\text{DOF}$	$L$	$\beta_G/\nu$	$\chi^2/\text{DOF}$
10 – 64	1.237(7)	1.21	12 – 64	1.244(8)	1.13
10 – 56	1.235(7)	1.26	12 – 56	1.241(9)	1.22
10 – 48	1.229(6)	0.88	12 – 48	1.234(9)	0.89
10 – 40	1.224(7)	0.77	14 – 64	1.258(7)	0.56
10 – 32	1.221(8)	0.90	14 – 56	1.257(8)	0.53
10 – 24	1.220(11)	1.12	16 – 64	1.258(9)	0.60
10 – 20	1.213(15)	1.36	16 – 56	1.256(10)	0.68

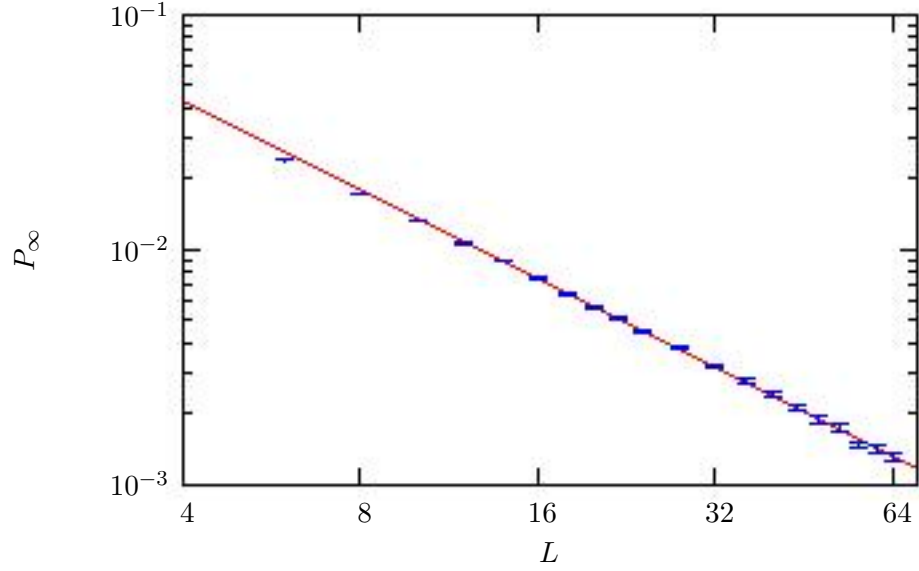


FIG. 9: Log-log plot of the percolation strength  $P_\infty$  of the XY HT graphs at the percolation threshold (25) as a function of the lattice size  $L$ . The straight line is obtained through a two-parameter fit in the interval  $L = 10 - 64$ .

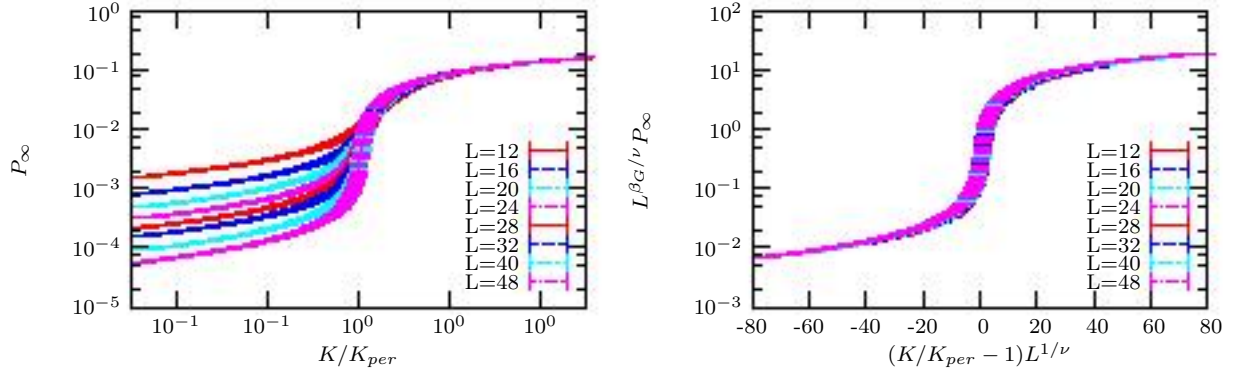


FIG. 10: Collapse of the XY percolation strength data measured on lattices of different size  $L$  (left panel) when  $L^{\beta_G/\nu} P_\infty$  is plotted as a function of  $(K/K_{\text{per}} - 1)L^{1/\nu}$  (right panel) on a semilogarithmic scale.

$$D = 1.7626(66) \quad (27)$$

for the fractal dimension of XY HT graphs at the percolation threshold. Comparison with the estimate (22) for the fractal dimension of the Ising HT graphs shows that the XY graphs are more crumpled although still much less so than a Brownian random walk. For the graph

distribution exponent  $\sigma$  we arrive at the estimate

$$\sigma = 0.8446(45), \quad (28)$$

which is lower than the estimate (23) for the Ising model. Our estimate (27) is in good agreement with the value  $D = 1.7655(20)$  recently reported by Prokof'ev and Svistunov [4] for the  $|\phi|^4$  theory which they obtained using their worm algorithm [6]. As stated in the Introduction, the HT graphs of that model as well as the worm update algorithm used to simulate them are completely different from the XY HT graphs and the plaquette update. Yet, despite these differences, the fractal dimensions of the two models, which share the same universality class, agree within error bars. We take this as a strong indication that, as expected, universality holds for the fractal structure of HT graphs.

## V. CONCLUSIONS

In this paper, it was shown that the geometric Monte Carlo approach originally introduced in the context of 2D spin models [2], in which HT graphs are simulated directly and analyzed with the help of percolation observables, can also be applied to 3D spin models. The 3D Ising HT graphs were shown to percolate right at the critical temperature, which is known to high precision. The phase transition to the ordered, low-temperature state in this spin model was shown to be reflected by a proliferation of HT graphs. Also, through data collapse, it was shown that the diverging length scale relevant to the HT graphs in the vicinity of the percolation threshold is the spin correlation length. With the help of finite-size scaling, the fractal dimensions of the closed Ising and XY HT graphs were determined as in percolation theory. Both models are handled similarly, with the only difference that, in contrast to the Ising HT graphs, the XY HT graphs are oriented. Finally, it was shown that universality holds for the fractal structure of HT graphs.

- 
- [1] *Series Expansions for Lattice Models*, edited by C. Domb and M. S. Green, *Phase Transitions and Critical Phenomena*, Vol. 3 (Academic Press, New York, N.Y., 1974).
  - [2] W. Janke and A. M. J. Schakel, Nucl. Phys. B [FS] **700**, 385 (2004).
  - [3] W. Janke and A. M. J. Schakel, Phys. Rev. Lett. **95**, 135702 (2005).

- [4] N. Prokof'ev and B. Svistunov, Phys. Rev. Lett. 96, 219701 (2006).
- [5] W. Janke and A. M. J. Schakel, *Anomalous Scaling and Fractal Dimensions*, cond-mat/0508734 (2005).
- [6] N. V. Prokof'ev and B. V. Svistunov, Phys. Rev. Lett. **87**, 160601 (2001)
- [7] H. E. Stanley, *Introduction to Phase Transitions and Critical Phenomena* (Oxford University Press, New York, 1971).
- [8] H.-M. Erking, *A new cluster algorithm for the Ising model*, Diplomarbeit, Technische Universität Graz (2000).
- [9] A. M. Polyakov, *Gauge Fields and Strings* (Harwood, New York, 1987).
- [10] D. Stauffer and A. Aharony, *Introduction to Percolation Theory*, 2nd edition (Taylor & Francis, London, 1994).
- [11] K. Binder and D. W. Heermann, *Monte Carlo Simulation in Statistical Physics* (Springer, Berlin, 1997).
- [12] H.W.J. Blöte, L.N. Shchur, and A.L. Talapov, Int. J. Mod. Phys. C **10**, 1137 (1999).
- [13] M. Campostrini, A. Pelissetto, P. Rossi, and E. Vicari, Phys. Rev. E **65**, 066127 (2002).
- [14] R. Guida and J. Zinn-Justin, J. Phys. A **31**, 8103 (1998).
- [15] M. Campostrini, M. Hasenbusch, A. Pelissetto, and E. Vicari, Phys. Rev. B **74**, 144506 (2006).